NONDESTRUCTIVE IDENTIFICATION OF MILLET VARIETIES USING HYPERSPECTRAL IMAGING TECHNOLOGY

X. Wang, Z. Li *, D. Zheng *, W. Wang

College of Engineering, Shanxi Agricultural University,
Taigu, 030801, China; e-mail: lizhiweitong@163.com; zhengdecong@126.com

In this study, we used eight millet varieties and took visible-near infrared hyperspectral images of 480 millet samples. Spectral and image characteristics, including texture and color features, of the millet samples, were extracted from the hyperspectral images. Support vector machine (SVM) models for millet variety identification were established using the extracted spectral and image characteristics. An attention-Convolutional recurrent neural network (attention-CRNN) model with attention mechanism was introduced for the identification of millet varieties, and the SVM and attention-CRNN models for millet variety identification were established using an image and spectral features fusion method. We found that the highest mathematical transformation method was the reciprocal logarithmic method. The identification accuracy of the SVM cultivar classification model with the reciprocal logarithmic spectral characteristics curve was 73.13%. The overall identification accuracy of the SVM model for the eight millet varieties using the image features was only 61.25%. The identification accuracy of the SVM model using the image and spectral information fusion method greatly improved the overall accuracy rate to 77.5%, and the minimum discrimination accuracy of the millet varieties increased from 50 to 65%. The overall identification accuracy of the attention-CRNN model was 87.50%, which is 10% higher than that of the SVM model, and the minimum discrimination accuracy of the millet varieties increased from 65 to 90%. The results show that the attention-CRNN model improved the overall identification accuracy of the eight millet varieties and greatly improved the minimum identification accuracy. The attention-CRNN model shows great potential for the nondestructive identification of millet and possibly other small grain varieties.

Keywords: *hyperspectral imaging, millet, convolutional recurrent neural network, attention mechanism.*

НЕРАЗРУШАЮЩАЯ ИДЕНТИФИКАЦИЯ СОРТОВ ПРОСА НА ОСНОВЕ ТЕХНОЛОГИИ ГИПЕРСПЕКТРАЛЬНОЙ ВИЗУАЛИЗАЦИИ

X. Wang, Z. Li *, D. Zheng *, W. Wang

УДК 543.42:664.788.4

Аграрный университет Шаньси,
Тайгу, 030801, Китай; e-mail: lizhiweitong@163.com; zhengdecong@126.com

(Поступила 10 декабря 2018)

Изучены гиперспектральные изображения 480 образцов проса восьми сортов в видимой и ближней инфракрасной областях спектра. В результате анализа изображений получены спектральные и графические характеристики образцов проса, выявлены особенности текстуры и цвета. На основе полученных характеристик созданы модели опорных векторов (SVM) для идентификации сортов проса. Идентификация сортов проса проведена на основе конволюционной рекуррентной нейронной сети (attention-CRNN), включающей в себя механизм внимания, а также с помощью моделей SVM и attention-CRNN методом слияния изображений и спектральных признаков. Определено, что лучшим методом преобразования является обратно-логарифмический метод. Точность идентификации сортов проса на базе классификационной модели SVM с обратно-логарифмической кривой спектральных характеристик 73.13%. Средняя точность идентификации восьми сортов проса по модели SVM с помощью признаков изображения 61.25%. Точность идентификации по модели SVM с использованием метода слияния изображения и спектральной информации значительно повышает

общий показатель точности до 77.5%, а минимальная точность распознавания сортов проса увеличивается с 50 до 65%. Средняя точность идентификации по модели attention-CRNN 87.50%, что на 10% выше, чем у модели SVM, а минимальная точность распознавания сортов проса увеличивается с 65 до 90%. Использование модели attention-CRNN улучшает общую точность идентификации восьми сортов проса и значительно увеличивает минимальную точность идентификации. Модель attention-CRNN представляет большой интерес для неразрушающей идентификации проса и, возможно, других мелких сортов зерна.

Ключевые слова: *гиперспектральная визуализация, просо, конволюционная рекуррентная нейронная сеть, механизм внимания.*

Introduction. Millet is one of the "five grains" (millet, rice, wheat, soybean, and sorghum) that were important in ancient China and it remains one of the largest crops in China. Millet is rich in vitamins, minerals, and dietary fiber and because of its high nutritional value is a very popular crop [1]. Traditional seed detection methods include artificial detection, protein electrophoresis identification, DNA molecular markers, and field identification [2]. However, these methods have many shortcomings, such as long identification times, low accuracy, and the need to destroy the seed. Therefore, the realization of a rapid nondestructive method for identifying millet varieties has become an important research target.

Hyperspectral imaging technology is a new nondestructive testing technology that combines image and spectral information, and it has been widely used in the identification and quality nondestructive testing of agricultural products [3, 4]. Ding et al. [5] used hyperspectral technology and a Bayes discriminant analysis method to establish a discriminant model for wheat grain; the accuracy of the model was 98%. Wu et al. [6] established a new model with a discriminant accuracy of 70.8% by collecting hyperspectral reflectance images of four varieties of maize seeds and combining them with a partial least square method. Ten kinds of hyperspectral images of rice seed were collected by Deng et al. [7], and a discriminant model with 96% accuracy was established by fusing spectral and image feature information. The hyperspectral data of normal and imperfect wheat grains were collected by Yu et al. [8], and a convolutional neural network (CNN) classification model was established, with the recognition rate for a test set of 99.98%.

Most of the current research is focused on the classification of large grain varieties, so small-grain cereals such as millet have been somewhat overlooked. Most classification methods are based on original spectral information and its mathematical transformation, whereas classification methods based on spectral and image characteristics are limited. The main modeling methods are CNN and recurrent neural network (RNN), and attention-convolutional recurrent neural network (attention-CRNN) models have been used less.

In this study, we used eight millet varieties and obtained hyperspectral images of 480 millet samples using visible-near infrared hyperspectral imaging technology. The spectral and image characteristics, which included texture and color features of the millet samples, were extracted from the hyperspectral images. A support vector machine (SVM) millet cultivar identification model was established using the spectral and image characteristics, and SVM and attention-CRNN millet cultivar identification models were established using an image and spectral features fusion method. The aim of the study was to find a rapid and nondestructive identification method for small grain cereals such as millet.

Experimental. *Experimental samples.* Millet samples were obtained from the Millet Research Institute of the Shanxi Provincial Academy of Agricultural Sciences, China. The eight varieties were: Hongruan millet, Jin millet 28, Ji millet 39, Changnong 0301, Changnong 40, Dun millet 1, Jin millet 56, and Changnong 35. Sixty seeds were selected for each millet variety. The selection criteria were: seeds with intact appearance, full grain, and even head. Forty seeds were selected randomly as the modeling set, and the remaining 20 seeds were used as the prediction set. The total number of seed samples was 480; 320 were the modeling set and the remaining 160 were the prediction set.

Acquisition of hyperspectral images. We used a Starter Kit indoor mobile scanning platform (Headwall Photonics, USA) to take visible-near infrared hyperspectral images. The hyperspectral imaging system had an indoor moving scanning platform, a miniature near infrared hyperspectral imager (aperture 1.4, focal length 25 mm), a halogen lamp source, a controller, and a dedicated computer.

The acquisition parameters of the hyperspectral image data were: spectral range 380–1000 nm, incident slit width 30 μm, and spectral resolution 0.727 nm; the band number was 854. Because the spectral reflectance was disturbed by the equipment noise at both sides of the range (380 and 1000 nm), the bands at both sides were removed before modeling, so the spectral range used for modeling was 412.368–972.004 nm, and the band number were 771.

To reduce the interference of the noise caused by uneven distribution of the light source and the dark current noise [9], the system was calibrated before the experiment. The correction formula was as follows:

$$I = \left((I_0 - B)/(W - B)\right) \times 100, \quad (1)$$

where I is the corrected hyperspectral image, I_0 is the original hyperspectral image, W is the white background image captured by scanning a standard white correction board, and B is the dark background image captured by covering the lens. During the experiment, the acquisition system corrected the hyperspectral image automatically using the correction formula.

Hyperspectral image processing method. The hyperspectral image contained both spectral and image information of the millet samples, so we divided the hyperspectral image processing into two parts: spectral feature extraction and image feature extraction. The image area of the millet seed was picked from the image, and for each pixel in the millet region there was a corresponding diffuse reflectance spectrum curve. The spectral information of a sample was obtained using a statistical average method on the diffuse reflectance spectral curves of all the pixels in the image of the millet seed.

Extraction of image features. The image features that we selected were texture and color. The texture features reflect the gray-level properties in the image and the spatial topological relationship. Compared with morphological features, texture features contain more information on the physical and chemical properties of a sample. The color feature reflects the surface properties of the millet samples.

The regions of interest of the grains were selected from the hyperspectral images and the images of single grains using ENVI 5.0 software. The texture and color features of a single millet grain were extracted using MATLAB 2007. The texture information of a millet hyperspectral image was extracted using a gray level co-occurrence matrix (GLCM) [10], the mathematical significance of which is the probability matrix of pixels with distance d in θ direction and gray scale i, j:

$$P(i,j,d,\theta) = \{[(x,y),(x + \Delta x, y + \Delta y)] | f(x,y) = i, f(x + \Delta x, y + \Delta y) = j\}, \quad (2)$$

where $i, j = \{0, 1, 2, 3, ..., k - 1\}$ and θ = 45, 90, 270, and 360°.

We set the gray gradation of the images to 16 and extracted seven common texture features: energy, entropy, moment of inertia, correlation, mean, standard deviation, and consistency. The RGB color system was used to extract six color features, namely, the mean and variance of the red, green, and blue components. Overall, the image features of the whole millet sample consisted of 13 parameters; 7 texture features and 6 color features.

Extraction and transformation of spectral features. We extracted the diffuse reflectance spectra of all pixels within the range of the single millet grain image using ENVI 5.0 software, and the average diffuse reflectance spectra were obtained using a statistical averaging method. Every millet grain sample corresponded to an average spectral curve. The average spectral curves of each millet variety were obtained using a mathematical average method.

To fully extract the effective information in the hyperspectral data, better highlight the reflection and absorption characteristics of the spectrum, and achieve better classification effects, we used four mathematical transformation methods to transform the spectral characteristic curves. The four mathematical transformation methods were reciprocal transformation, logarithmic transformation, logarithmic transformation of reciprocal, and first-order differential.

Spectral and image features fusion method. To fully use the acquired hyperspectral imaging data, the spectral, texture, and color features were mixed together. The data dimension after fusion was 784; the image information dimension was 13, and the spectral information dimension was 771. In the SVM model, because of the large differences in properties and values between the spectral and image features, if the extracted features are fused directly, the classification effect of the model may be affected by the heavy weight of some features or the less use of some other features. Therefore, we performed a principal component analysis (PCA) to extract the first 13 principal components (rate of cumulative contribution was >99%) from the 771-dimension spectroscopic data. For the first eight principal components (rate of cumulative contribution was >99%) extracted from the 13-dimensional image data, the 13-dimensional spectroscopic features and 8-dimensional image features after PCA dimensionality reduction were normalized followed by fusion in series. Finally, the fused feature vector of the 21 dimensions was taken as the input data for the SVM classification model. The CRNN model [11] can compress and dimension the data automatically, and the attention mechanism provided an intuitive explanation of the contribution of each feature to the classification results. Therefore, the 784-dimensional data after fusion were used directly to establish the attention-CRNN classification model.

Classification models. SVM and attention-CRNN were used to establish the classification model reported in this study.

SVM model. SVM [12] is a nonparametric classifier for finite samples. It is based on the principles of statistical learning and structural risk minimization and has good generalization and robustness. The basic idea is the mapping of the training data set to a high-dimensional space, then finding the optimal hyperplane in the high-dimensional space for the separation of sample set. SVM is used to solve the optimization process as

$$\min \frac{1}{2}\|w\|^2 + c\sum_{i=1}^{n}\varepsilon_i, \tag{3}$$

$$s.t.y_i(wx_i + b) \geq 1 - \varepsilon_i,\ \ \varepsilon_i > 0,\ \ i = 1, 2, 3, \ldots, n, \tag{4}$$

where ε_i is a Slack variable and c is a penalty. Lagrangian duality is applied to get the optimal solution by solving the dual problem. The function in the SVM algorithm for classification is as follows:

$$f(x) = \operatorname{sgn}\left(\sum_{i=1}^{n}\alpha_i y_i K(x_i, x) + b\right), \tag{5}$$

where α_i is a Lagrangian multiplier and $K(x_i, x_j)$ is a kernel function.

The selection of the kernel function is the key to improving the performance of the SVM model. The radial basis function (RBF) is used. The penalty factor c and the kernel function parameter g are the two key parameters of the RBF, and there is no unified optimal parameter in the SVM model for different training sets. Therefore, we applied cross-validation to optimize the selection of different training sets c and g.

Attention-CRNN model. The CNN and RNN have significant effects in classification models [13], but they also have some shortcomings: less intuitive and poor interpretability. The attention mechanism is a commonly used long-term memory mechanism that has been used in modeling in natural language processing. It can intuitively show the contribution of each piece of feature information to the results. We used the attention mechanism to establish the attention-CRNN classification model shown in Fig. 1.

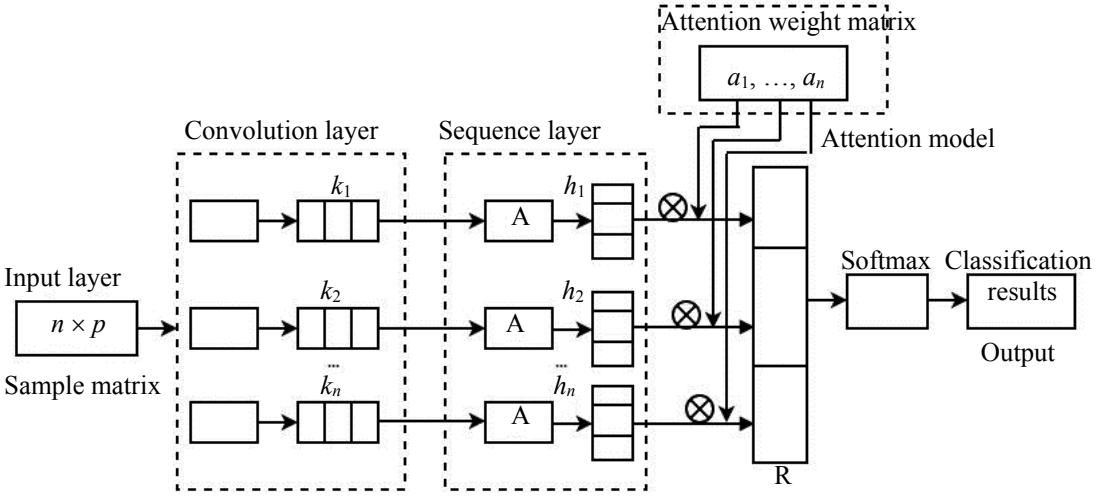

Fig. 1. Attention-CRNN structure.

The attention-CRNN model mainly comprises an input layer, convolution layer, sequence layer, and attention model. The input layer is a matrix X, which comprises $n \times p$ hyperspectral data, with n as the sample number and P as the spectral dimension. The convolution layer is the sample feature extraction layer. The input sample matrix X is convoluted by the convolution kernel with size of $m \times d$ to obtain the characteristic value g_i

$$g_i = f(w \times X_{i:i+h-1} + b), \tag{6}$$

where f is the activation function, b is the bias item, and $X_{i:i+h-1}$ is the feature extracted from line i to $i+h-1$ of X and expressed as $G = [g_1, g_2, \ldots, g_n]$. The sample eigenvector expressed as $K = [k_1, k_2, \ldots, k_n]$ is obtained by the maximum pooling treatment of the next sampling layer. The eigenvector $k_1, k_2, \ldots, k_n$ is the input value of the third-level RNN. After iterations, the hidden layer vectors $h_1, h_2, \ldots, h_n$ are obtained.

We introduced the attention mechanism [14] to better explain the importance of each sample feature. In this model, each hidden node in the RNN layer was assigned an attention weight [15], where the greater the weight, the more important is the influence of the feature on the classification of millet varieties. The formula was as follows

$$u_t = \tanh(W_w h_i + b_w), \tag{7}$$

$$a_i = \frac{\exp(u_w^T u_i)}{\sum_{i=1}^{n} \exp(u_w^T u_i)}, \tag{8}$$

where h_i is the implicit vector that corresponds to node i in the RNN layer, u_i is the implicit vector in the attention layer, W_w and b_w are the coefficient matrix and bias vector, respectively and a_i is the attention weight of node i in the RNN and satisfies $\sum_{i=1}^{n} a_i = 1$, where n is the number of millet samples and u_w is initialized randomly and continuously changes in the training process.

The attention weight matrix and the corresponding hidden layer vector in the RNN layer are dotted with each other to complete the weighting to get the final feature vector R:

$$R = \sum_{i=1}^{n} a_i h_i. \tag{9}$$

The eigenvector R of sample X is used as the final eigenvector to be input into the soft-max layer. A dropout strategy was used to prevent overfitting.

By mining the features of the sample data using a depth neural network, the attention mechanism was introduced to obtain the attention-CRNN model. This model with the attention mechanism should be adaptive to perceive the features related to specific tasks, explain the importance of features of classification intuitively, and effectively improve the accuracy of the classification.

Results and discussion. *Results of hyperspectral image processing.* The image features and spectral characteristics of the millet samples were obtained by processing the hyperspectral images. The image features of the samples of the eight millet varieties are shown in Fig. 2a. The abscissa coordinates expressed in order from small to large were energy, entropy, moment of inertia, correlation, mean, standard deviation, consistency, and mean and variance of the red, green, and blue components. The average spectral curve is shown in Fig. 2b.

As shown in Fig. 2a, the trend of image characteristics of Hongruan millet was different from that of the other varieties. Compared with the other millet varieties, Hongruan millet was obviously lower in average value, standard deviation, green mean value, blue mean value, green variance, and blue variance. Therefore, the accuracy of classification of Hongruan millet using the image features is likely to be high. Jin millet 56 and Changnong 35 had the same trend and several overlaps, indicating they might interfere with each other's classification and influence the classification effect. The overlaps of some eigenvalues were detected among other cultivars, so it might be difficult to easily distinguish them. These results indicate that the accuracy of classification using only image features may be low.

The visible/near infrared band used in this study reflected mainly the absorption of O–H, C–H, and other chemical bonds in millet. It was the main band that reflected the differences of chemical composition and physical state of the seeds. The average spectral curve showed the difference of the eight millet varieties in these bands (Fig. 2b). Within the range 476–550 nm, the change of Hongruan millet was obviously different from those of the other varieties, and the spectral reflectance was lower than that of the other varieties; in the range 620–1000 nm, the reflectance of Jin millet 28 was significantly lower than that of the other varieties. This suggested that the correct rate of identification of Hongruan millet and Jin millet 28 would be high using spectral information, whereas the spectral curves of Changnong 0301 and Dun millet 1 were basically the same. There was obvious overlap between 720 and 900 nm, which resulted in mutual interference in the classification process, and the identification accuracy might be low.

SVM model with spectral characteristic curve transformation. We used the original spectral characteristic curve and its spectral data after the four mathematical transformations to establish the SVM discriminant model. By cross-validation, when the values of c and g were determined to be 16 and 0.25 respectively, the discriminant results of the SVM model for the prediction set are shown in Table 1.

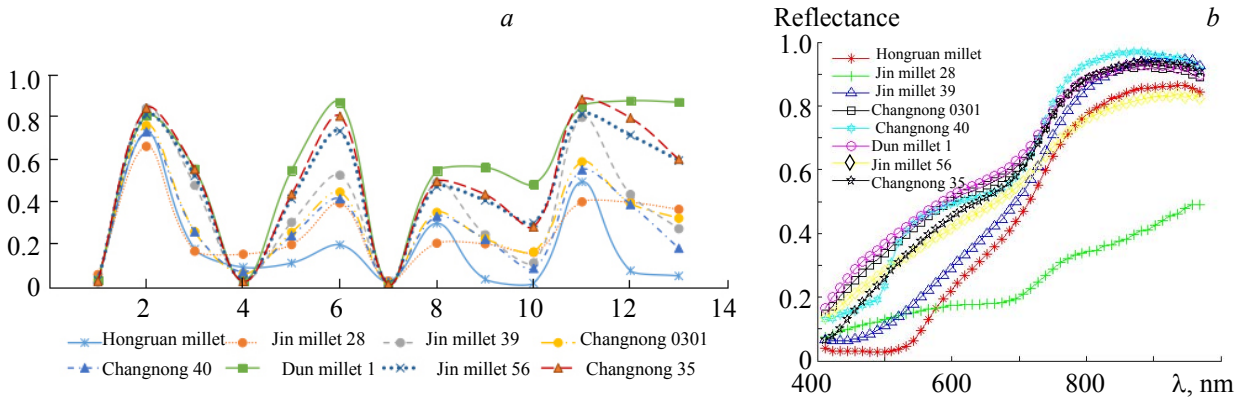

Fig. 2. Image features (a) and average spectral curves (b) of 8 kinds of millet.

TABLE 1. Results of the SVM Model in the Spectral Feature Curve Transformation Methods

Spectral transformation	Accuracy, %
Original spectrum	70.63
Reciprocal spectrum	65
The logarithmic spectrum	65.63
Reciprocal logarithmic spectrum	73.13
The first derivative spectrum	66.25

Compared with other models, the SVM classification model based on the reciprocal logarithmic spectral characteristic curve had the highest discrimination accuracy (73.13%). This may be because the spectral reflectance, which was transformed by the reciprocal logarithm, improved the resolution of overlapping spectral bands, enhanced spectral differences, reduced the influence of multiplicative factors caused by illumination changes and improved the discrimination rate of the model. Therefore, the reciprocal logarithmic spectral characteristic curves were used in the follow-up study.

SVM model with image features. We established the SVM classification model based on seven texture features and six color features of the millet grains. We obtained the discriminant results of the prediction set using cross-validation with values of c and g determined to be 32 and 1 respectively, as shown in Table 2.

TABLE 2. Results from the SVM Model Using Image Features

Species	Sample number	Correct number	Erroneous number	Correct rate, %
Hongruan millet	20	15	5	75
Jin millet 28	20	12	8	60
Ji millet 39	20	11	9	55
Chang Nong 0301	20	14	6	70
Chang Nong 40	20	11	9	55
Dun millet 1	20	12	8	60
Jin millet 56	20	10	10	50
Chang Nong 35	20	13	7	65
Total	160	98	62	61.25

As shown in Table 2, the highest classification accuracy of the SVM classification model based on image features was 75%. Because Hongruan millet showed large differences from the other millet varieties (Fig. 2, a), the classification accuracy was highest for this variety. The identification accuracy for the other millet varieties was <70%, and the identification accuracy for Jin millet 56 was lowest at only 50%. This may be because of the similarity of texture and color features among the millet varieties, which affected the discrimination accuracy. The average classification accuracy of SVM classification model on the eight millet

varieties was only 61.25%. Although hyperspectral image features could reflect the differences among millet varieties, the accuracy was low when only image information was used to establish the classification model. Therefore, the fusion of image and spectral information for modeling might give better classification and identification results.

Attention-CRNN model with the fusion of image and spectral features. The fusion of spectral information and image information data were input into the attention-CRNN model to classify the millet varieties. The specific parameters of the model were set up with two convolution layers in the convolution neural network. The first layer contained 18 convolution kernels with a size of 5×5, and the second layer contained 24 convolution kernels with a size of 3×3. Different convolution kernels were used to convolute all the feature maps in the former layer, then the corresponding elements were accumulated and biased and each output feature map was activated using the ReLu function. ReLu was activated by the zero-threshold matrix, which to some extent prevented gradient disappearance and expedited the convergence speed of the network as follows:

$$f(x) = \max(x, 0), \begin{cases} x > 0, f(x) = x \\ x < 0, f(x) = 0 \end{cases}. \tag{10}$$

The size of pooling layer was 2×2; the dimension of hidden layer vectors and attention layer eigenvectors in the third-layer RNN were both set to 100. To prevent overfitting, the dropout layer was inserted in the soft-max layer with a parameter of 0.5. The mini-batch gradient descent method was used in the model. The network learning rate was 0.5, the batch was 20, and the maximum number of iterations was set to 6000. The loss function curve and accuracy value were used as the basis of convergence. The overall discriminating accuracy of the model for the 160 prediction sets was 87.5%. The 21-dimension feature fusion data (13-dimensional spectral data and 8-dimensional image data) processed by PCA were used as the input data to establish the SVM model after the cross-validation, when the final values of *c* and *g* were 32 and 0.5.

The identification results of the attention-CRNN and SVM models for the prediction set are shown in Table 3. The results in Table 3 show that the overall accuracy of the SVM model based on image and spectral information fusion was 77.50%. The overall accuracy of the SVM model increased by about 4.37% compared with the SVM model using only the spectral information, and by 16.25% compared with the SVM model using only the image information. The minimum discrimination accuracy of millet varieties increased from 50 to 65%, which indicates that using the image and spectral information fusion method improved the identification accuracy of millet varieties.

TABLE 3. Sample Recognition Rate of the Attention-CRNN and SVM Models

Species	Attention-CRNN model, %	SVM model, %
Hongruan millet	95	90
Jin millet 28	90	80
Ji millet 39	80	70
Chang nong 0301	85	75
Chang nong 40	95	80
Dun millet 1	80	75
Jin millet 56	90	65
Chang nong 35	85	85
Total	87.50	77.50

The overall accuracy of the attention-CRNN model was 87.50%, which was 10% higher than that of the SVM model. The identification accuracy of Jin millet 56 using the attention-CRNN model was 90%, an increase of about 25% compared with the SVM model. The identification accuracies of Changnong 40 increased by 15%, and those of Jin millet 28, Ji millet 39, and Changnong 0301 increased by 10% using the attention-CRNN model, and the minimum discrimination accuracy of millet varieties increased from 65% to 90%. These results show that the attention-CRNN model could better highlight important features, alleviate the loss of information, and had good feature extraction ability. We expect that the attention-CRNN model could improve the overall identification accuracy of cereal varieties and greatly improve the minimum identification accuracy.

Conclusion. Eight millet varieties were selected, and visible-near infrared hyperspectral images of 480 millet samples were taken. Spectral and image characteristics, including texture and color features, of the millet samples were extracted from the hyperspectral images. SVM millet variety identification models were established using spectral and image features. SVM and attention-CRNN millet variety identification models were established using an image and spectral features fusion method. The identification results of the various modeling methods were analyzed in this study. The conclusions were as follows.

The identification accuracy of the SVM classification model based on a reciprocal logarithmic spectral characteristic curve was 73.13%, which was the highest value among the four mathematical transformation methods. The overall identification accuracy of the eight millet varieties with the SVM classification model using image features was only 61.25%. The identification accuracy of the SVM model using image and spectral information fusion was 77.50%, enhancements of about 4.37% compared with the SVM model using only spectral information and 16.25% compared with the SVM model using only image information. The minimum discrimination accuracy of the millet varieties increased from 50 to 65%.

The attention-CRNN model with attention mechanism was developed to accurately identify millet varieties. The overall accuracy of the attention-CRNN model was 87.50%, which is 10% higher than the overall accuracy of the SVM model. The minimum discrimination accuracy of millet varieties increased from 65 to 90%. The attention-CRNN model has good feature extraction ability and improved the identification accuracy of millet varieties. The attention-CRNN model shows great potential for the nondestructive identification of millet and possibly other small grain varieties. To meet the needs of practical applications, the further development of models with higher discrimination accuracy and with fewer bands and a band selection algorithm are required.

Acknowledgment. This work was supported by grants from the National Key Research and Development Program of China (2017YFD0701501), General Program of National Natural Science Foundation of ShanXi Province (201701D121099), and Science and Technology Innovation Fund of Shanxi Agricultural University (2017YJ12).

REFERENCES

1. X. M. Diao, R. H. Cheng, *Sci. Agric. Sin.*, **50**, 4469–4474 (2017).
2. X. Ke, M. Z. Du, *J. Image Graphics*, **21**, 24–38 (2016).
3. A. M. Rady, D. E. Guyer, W. Kirk, I. R. Donis-González, *J. Food Eng.*, **135**, 11–25 (2014).
4. M. A. Teena, A. Manickavasagan, L. Ravikanth, D. S. Jayas, *J. Stored Prod. Res*., **59**, 306–313 (2014).
5. Q. Ding, Z. X. Shu, H. Y. Zhao, C. H. Yin, Y. Cao, *Grain Storage,* **46**, 30–35 (2017).
6. X. Wu, W. Z. Zhang, J. F. Lu, Z. J. Qiu, Y. He, *Spectrosc. Spectr. Anal.*, **36**, 511–514 (2016).
7. X. Q. Deng, Q. B. Zhu, M. Huang, *Laser Optoelectron. Progr.*, **52**, 128–134 (2015).
8. C. C. Yu, L. Zhou, X. Wang, J. Z. Wu, Q. Liu, *Food Sci.*, **38**, 283–287 (2017).
9. A. Ambrose, L. M. Kandpal, M. S. Kim, W. H. Lee, B. K. Cho, *Infrared Phys. Technol.*, **75**, 173–179 (2016).
10. M. I. A. P. Zamri, F. Cordova, A. S. M. Khairuddin, N. Mokhtar, R. Yusof, *Comput. Electron. Agric.*, **124**, 227–233 (2016).
11. B. Zhao, X. L. Li, X. Q. Lu, Z. G. Wang, *Neurocomputing*, **322**, 47–57 (2018).
12. A. J. Smola, B. Schòlkopf, *State Comput*., **14**, 199–222 (2004).
13. X. J. Guo, L. Chen, C. Q. Shen, *Measurement*, **93**, 490–502 (2016).
14. Y. Z. Ji, H. J. Zhang, Q. M. Jonathan Wu, *Neurocomputing*, **322**, 130–140 (2018).
15. A. K. Bhunia, A. Konwer, A. K. Bhunia, A. Bhowmick, P. P. Roy, U. Pal, *Pattern Recogn.*, **85**, 172–184 (2019).